The Intensity as a Function of Temperature of the Low-Angle X-Ray Diffraction Maxima of the $\underline{n}$-Paraffins: Hexatriacontane, Tetratetracontane, and Tetranonacontane

Peter K. Sullivan* and James J. Weeks

Institute for Materials Research, National Bureau of Standards, Washington, D.C. 20234

The diffraction of x-rays by the crystalline n-paraffins, $C_{36}H_{74}$, $C_{44}H_{90}$, and $C_{94}H_{190}$, was examined at small angles—below seven degrees 2θ—as a function of temperature. The Bragg maxima (00l) that occur at these angles result from a lamellar repeat distance which depends on the molecular length. In general the intensity of these maxima was found to increase with increasing temperature in an approximately reversible manner. All the samples experienced solid-solid phase transitions in the temperature range of observation. Several possible mechanisms consistent with the temperature dependence of the intensity are considered.

Key words: Defects; n-paraffins; phase transition; temperature dependence; x-ray diffraction.

1. Introduction

Some polymers which exhibit high crystallinity [1, 2][1] display low-angle x-ray diffraction maxima which correspond to a lamellar repeat distance. In the case of linear polyethylene and a number of other polymers, it has been observed [3–5] that the intensities of the low-angle maxima increase with increasing temperature and that this phenomenon occurs reversibly.

Normally, one expects that the intensity of x-ray diffraction maxima from crystalline solids should decrease with increasing temperature. This is evidenced by the Debye-Waller factor [6] in structure calculations and in the experimental observation of the change in intensity of the diffraction maxima with temperature for a variety of solids [7].

The question which arises is whether the intensity behavior of the low-angle maxima with temperature is unique to these crystalline polymers or occurs in other compounds, such as the long-chain n-paraffins. Both the paraffins and polyethylene have the same —CH$_2$— repeat unit; however, a pure paraffin is essentially a single molecular species, while the polymer has a broad distribution in molecular weights. Both systems crystallize as lamellae, with very similar crystallographic subcells [8–12]. However, the basal surfaces of the paraffin lamellae are composed of methyl groups, while in the polymer lamellae these end surfaces are composed of more or less regular chain-folds [1].

In this article we present our observations of the intensities of the low-angle x-ray diffraction maxima as a function of temperature for three crystalline n-paraffins: n-$C_{36}H_{74}$, n-$C_{44}H_{90}$, and n-$C_{94}H_{190}$. We also discuss some possible causes of the observed intensity changes with temperature.

2. Experimental Detail

2.1. Apparatus

Diffraction intensities at angles up to $7°$ in 2θ were obtained using nickel-filtered copper radiation. The detector system consisted of a scintillation counter, pulse-height analyzer, and printer. A Kratky low-angle camera[2] with a $120\ \mu$ entrance slit was used for beam collimation. The detector slit width was commonly $270\ \mu$ and the sample to detector distance was 238.7 mm. Scanning was accomplished automatically with a Kratky step-scanner. Generally a counting time of 1 min was used at each angle. No slit-smearing corrections were made. The samples were contained either in a 1.5 mm diam glass capillary (0.01 mm wall thickness) or in a stainless steel holder ($25 \times 2.5 \times 3$ mm³) with beryllium foil sides. The capillary tube or holder was held in a small oven which had beryllium windows and $\frac{1}{2}$ in thick balsa wood insulation. Temperature control was achieved with a thermistor system which could maintain a constant sample temperature above

---

[1] Figures in brackets indicate the literature references at the end of this paper.

[2] Certain commercial materials and equipment are identified in this paper in order to specify adequately the experimental procedure. In no case does such identification imply recommendation or endorsement by the National Bureau of Standards, nor does it imply that the material or equipment is necessarily the best available for the purpose.

room temperature to within 0.1 K for a period of several days. Below room temperature the sample container was cooled with a stream of gas from liquid nitrogen; dry nitrogen gas (warmed) was blown across the beryllium windows to prevent ice formation. Temperature control was not as good as under these conditions, but constancy to ± 0.1 K could be maintained during the diffraction scan, which typically lasted about 90 min.

When the sample was inhomogeneous with respect to thickness or crystallite orientation small adjustments in the height of the oven above the optical bench were necessary to keep the same portion of the sample in the x-ray beam as the temperature was changed. It was found that an observation of the intensity of the $(00l)$ Bragg maximum as the sample was moved gave a profile of the inhomogeneities, so that a local maximum or minimum of intensity could be used as a reference point at any temperature.

2.2. Samples

a. Tetranonacontane, $n\text{-}C_{94}H_{190}$ (mp 387.4 K [13])

This compound was synthesized by Reinhard [13] and a sample was kindly supplied to us by Dr. John Crissman,[3] who had crystallized it from the melt in a Bridgman apparatus [14] (4 K gradient; drop rate of 0.4 mm/hr). The resulting polycrystalline sample was found to be highly oriented by examination with an
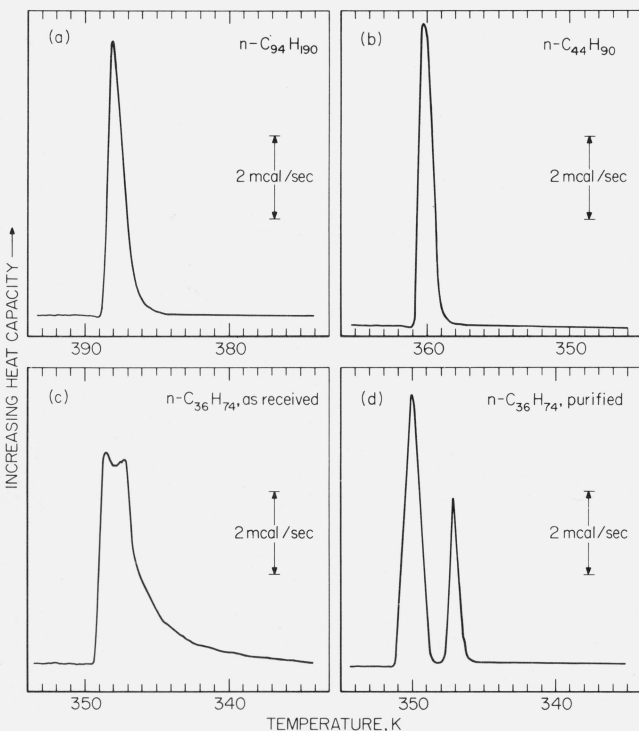

FIGURE 1. *Differential scanning calorimeter traces of the melting of (a)* n-C$_{94}$H$_{190}$, *as received, (b)* n-C$_{44}$H$_{90}$, *(c)* n-C$_{36}$H$_{74}$, *as received, and (d)* n-C$_{36}$H$_{74}$ *after purification as described in the text.*

The lower temperature peak in $n\text{-}C_{36}H_{74}$ is a solid-solid transition to the hexagonal phase. Heating rate was 2.5 deg/min in each case.

[3] Metallurgy Division, National Bureau of Standards, Washington, D.C. 20234.

x-ray camera having pinhole collimation. The diffraction spots of the long spacing showed no arcing. A Differential Scanning Calorimeter (DSC) scan of this sample—to be called "C$_{94}$ (orig)"—is shown in figure 1(a).

In order to estimate the effect of slit-smearing on the low-angle d-spacings obtained with the Kratky camera, part of the $n\text{-}C_{94}H_{190}$ sample was melted into a 1.5 mm thin-walled capillary tube and crystallized with approximately random orientation of the lamellae. Measurements on this sample will be designated, "C$_{94}$ (m. c.)".

Orthorhombic $n\text{-}C_{94}H_{190}$ may be obtained by crystallization from dilute solution [12]. Samples were prepared from butyl acetate and from xylene. In the former case, a 0.06 wt percent solution was very slowly cooled from 377 K. Precipitation occurred above 350 K. Using a phase-contrast optical microscope the crystals were observed to be growth spirals on twinned laths, typically about ten layers thick. The acute angle between adjacent (110) faces was found to be 66.3 deg, in agreement with what one calculates for the orthorhombic unit cell [12]. The sample was separated by filtration, dried at room temperature under high vacuum and cut into strips, which were compacted at a pressure of approximately 400 psi. This produced a semioriented sample or mat, as was evidenced by examination in the pinhole camera. The mat was then placed in the steel holder for subsequent x-ray examination and will be referred to as "C$_{94}$ (s. c.)".

The second solution-grown sample of $n\text{-}C_{94}H_{190}$ was prepared by cooling a 0.2 wt percent xylene solution from 383 K to room temperature. Crystallization occurred near 340 K. The sample was filtered and dried, and the mat cut into strips, which were examined without being compacted. This sample was annealed overnight at 382 K, after which time the lamellar d-spacing at 382 K indicated that the substance was no longer in a pure orthorhombic phase. This sample will be designated "C$_{94}$ (annealed)".

b. Tetratetracontane, $n\text{-}C_{44}H_{90}$ (mp 359.6 K [15])

This compound was synthesized by Clark [16] and a sample was made available to us by Dr. Crissman. A DSC scan of the original sample is shown in figure 1(b). A 0.34 wt percent toluene solution of the $n\text{-}C_{44}H_{90}$ was prepared and the sample crystallized by cooling from 329 to 289 K; precipitation began at 312 K. The toluene was removed by filtration and the crystal mat dried under vacuum at room temperature for 3.5 days. For x-ray examination, the mat was cut into strips and stacked in the steel holder parallel to the x-ray beam.

c. Hexatriacontane, $n\text{-}C_{36}H_{74}$ (mp 348.7 K [9])

The $n\text{-}C_{36}H_{74}$ was obtained commercially with a stated purity of 97 percent. Measurements were made on the original material as well as on a sample which was purified both by recrystallization from dilute benzene solution and subsequent zone refinement for 35 days (15 zones at 7 mm/hr). Both samples were crystallized from the melt before x-ray examination.

DSC traces of the original and purified samples are shown in figures 1(c) and 1(d) respectively. By comparison one sees that most of the impurities which broadened the transitions in the original material have been removed by the purification scheme.

For the case of n-$C_{36}H_{74}$ the preparation conditions were varied in an attempt to determine if there were any contribution of primary extinction to the intensity changes with temperature. Samples of n-$C_{36}H_{74}$ were crystallized under conditions which should lead to small and imperfect crystals. One sample was dissolved in toluene (0.15 wt %) and quenched by pouring the warm solution into a container which was at the temperature of a dry-ice acetone bath. A second sample was dissolved in ethanol and the solution atomized into a large beaker of rapidly stirred ice water. Each of these samples was dried at room temperature and subsequently ground at the temperature of dry ice.

2.3. Data Treatment

The low-angle x-ray diffraction maxima considered throughout this article correspond to the lamellar repeat distance, which in the case of the n-paraffins is determined by the length of a molecule.

The d-spacings were obtained from Bragg's law, $m\lambda = 2d \sin\theta$, where 2θ was measured from the peak positions of the primary beam and diffraction maximum. Because of smearing by the collimator and detector slits, most of the observed peaks were shifted toward smaller angles by amounts which depended on such variables as sample orientation and background intensity. Since the effect of smearing is angle dependent, being smaller at the larger angles, a more accurate determination of the d-spacings was obtained from the higher orders. Repeated scans on a given sample at constant temperature always gave agreement within 0.5 Å as long as no phase transformations occurred.

Unless noted otherwise the diffraction intensities reported are the integrated intensities obtained after subtracting a smooth scattering background from the observed intensities. The areas were determined by means of a planimeter. In cases where the lamellae were randomly oriented or where considerable void scattering was present, the location of the background was somewhat uncertain. However, a log-log plot of the scattered intensity against 2θ usually showed that a single, nearly linear background could be drawn under the first three orders of the d-spacing. For a given sample, the slopes of such lines were also noted to be independent of the temperature at which the scan had been made. Backgrounds from the log-log plots were transferred to linear plots and the areas then determined. Repeated x-ray scans of any sample at a given temperature always gave areas which agreed within 10 percent of each other.

3. Results

In general, the intensity effects we have observed on these n-paraffins were consistent with what has been observed in the case of polyethylene [3], that is to say,

the intensity of the low-angle $(00l)$ maxima increased substantially with increasing sample temperature. No broadening of the maxima was observed with the increase in intensities and the effects were found to be approximately reversible. The $(00l)$ d-spacings of our n-paraffins showed changes with temperature which were in part reversible. As will be seen shortly, these changes reflect the fact that solid-solid phase transformations are taking place in the paraffins at the higher temperatures of observation.

3.1. Tetranonacontane

The observed diffraction intensity from C_{94} (orig) at a temperature of 385.2 K—two degrees below its melting point—is shown in figure 2. Four orders of the low-angle d-spacing are shown; although, with our equipment six were observable at this temperature. The first two orders were defined by points taken every 0.00042 rad, the third and fourth orders with half as many points. There is little uncertainty in the background for this sample. Integrated intensities and d-spacings (assumed to be orders of the (001) spacing) are listed in table 1, as are the half-height widths of the maxima.

The x-ray diffraction from C_{94} (orig) was determined at five different temperatures and the observed intensities (with background subtracted) of the (001) spacing are shown in figure 3. The d-spacing as a function of temperature is shown in figure 4. It is seen that both the intensity and the d-spacing vary with temperature. In table 2 are listed the values of the (001) spacing
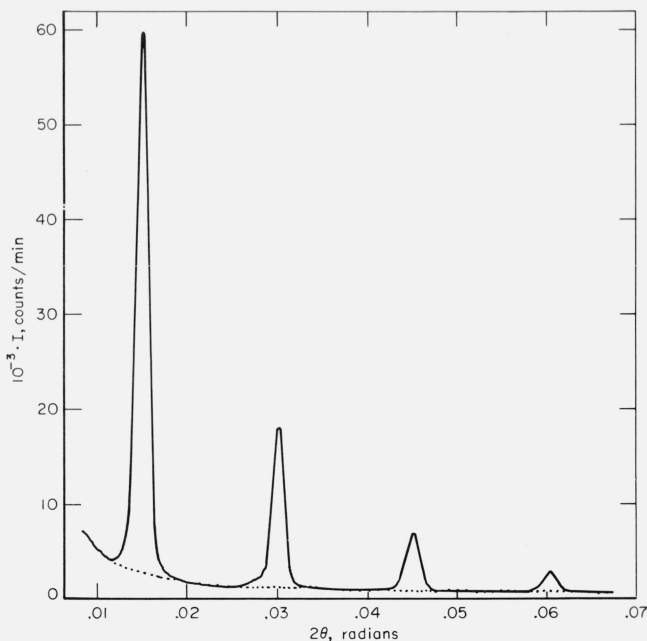
FIGURE 2. *The observed x-ray diffraction intensity as a function of the scattering angle from* n-$C_{94}H_{190}$, *as received, at a temperature of 385.2 K.*

The dotted line is the background intensity.

Order m	(001) spacing	Intensity	Half-height width[a]
	$\mathring{A}$	$cts \cdot rad \cdot min^{-1}$	rad
1	102.6	101.7	0.0015
2	102.4	29.7	.0016
3	102.6	11.3	.0016
4	102.3	4.3	.0017

[a] Instrumental half-height width, including the effect of sample thickness, is 0.0014 rad at the 1st order and 0.0016 rad at the 4th order.

and the integrated intensities of the first (I$_1$) and second (I$_2$) orders, given in the order in which they were obtained.

While the data shown in figures 2 and 3 appear to indicate that this sample of n-C$_{94}$H$_{190}$ is in a single

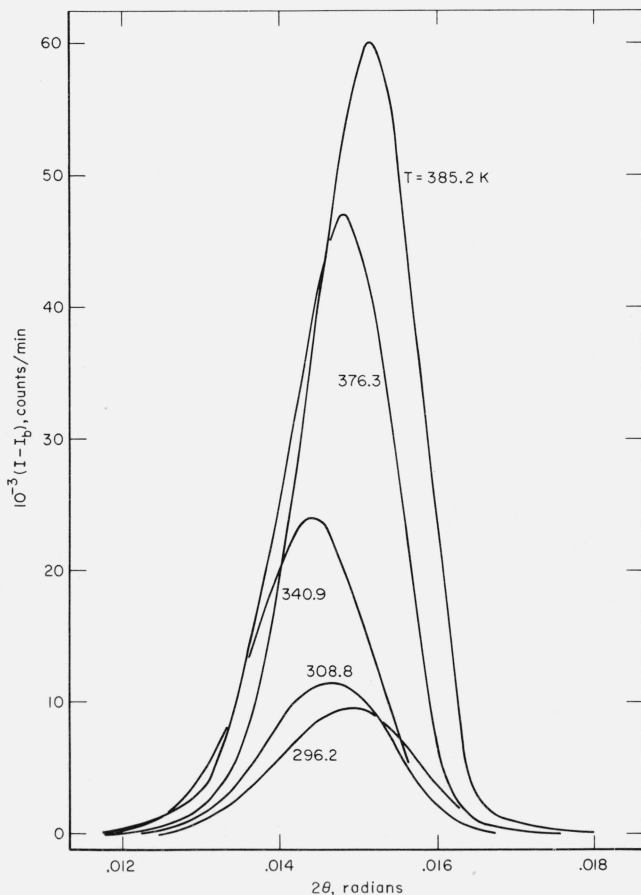FIGURE 3. *The observed diffraction intensity, after subtraction of the background intensity, from* n-C$_{94}$H$_{190}$ (orig) *at the temperatures shown as a function of scattering angle.*

The maximum in 2θ corresponds to the (001) spacing.
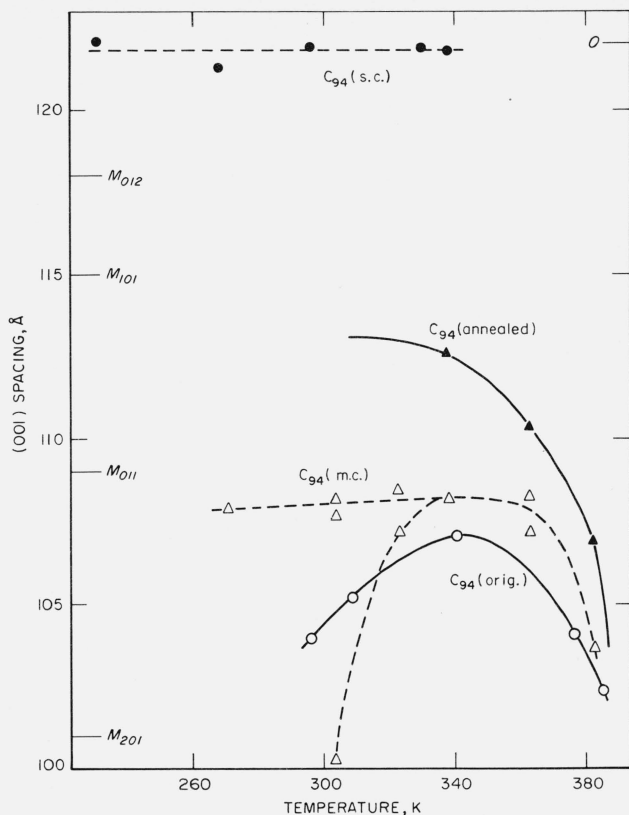

FIGURE 4. *The (001) spacings (obtained from the second order) of four different samples of* n-C$_{94}$H$_{190}$ *given as a function of temperature.*

Several *d*-values of possible monoclinic phases, M$_{hkl}$, are marked on the left margin; the value of the orthorhombic phase, 0, is indicated on the right.

crystalline phase, an examination of the sample in the pinhole-collimated camera established that this was not the case. The apparent single first order maximum could be resolved into two maxima, corresponding to spacings of 100.2 and 105.8 Å, which could arise from the two monoclinic forms reported by Wyckoff et al., 102 and 107 Å [17]. The first form may be obtained from the orthorhomic unit cell by translating each —CH$_2$— unit, in the adjacent molecule along the *a*-axis, by four —CH$_2$— units parallel to the *c*-axis [18, 19]. We designate this monoclinic form as M$_{201}$, where the subscript is the Miller subcell index of the plane formed by the terminal methyl groups. Similarly, the second form may be obtained from the orthorhombic unit cell by translating each —CH$_2$— unit, in the adjacent molecule along the *b*-axis, by two —CH$_2$— units parallel to the *c*-axis. We designate this form as M$_{011}$. It appears then that for this sample of n-C$_{94}$H$_{190}$, we could not resolve the individual monoclinic phases under the conditions of our slit camera. The calculated values of the (001) spacings of several possible monoclinic phases are given in table 3 for each of the three *n*-paraffins under investigation. They are based on literature values for the ortho-rhombic phase of each material.

TABLE 2. *Integrated intensities and values of (001) spacings for* n-$C_{94}H_{190}$, *listed in the order in which they were observed*

C_{94} (orig)

T	(001) spacing m=1	(001) spacing m=2	I_1	I_2
K	Å	Å	$\frac{cts \cdot rad}{min}$	$\frac{cts \cdot rad}{min}$
296.2	104.0	104.0	21	7.5
376.3	104.2	104.1	86	28.3
308.8	105.4	105.2	23	8.7
340.9	107.2	107.1	45	16.5
376.3	104.6		80	
385.2	102.6	102.4	102	29.7

C_{94} (s.c.)

T	m=1	m=2	I_1	I_2
296.0	123.1	121.9	19.8	6.7
268.2	122.9	121.3	19.0	6.4
231.3	123.1	122.1	18.2	6.0
296.1	122.7		20.4	
329.7	122.3	121.9	26.5	9.2
338.0	122.3	121.7	28.9	9.7

C_{94} (m.c.)

T	(001) spacing m=1	(001) spacing m=2	I_1	I_2
K	Å	Å	$\frac{cts \cdot rad}{min}$	$\frac{cts \cdot rad}{min}$
303.5	101.7	100.3	4.3	1.5
323.3	109.1	107.2	7.3	1.9
338.4	109.8	108.2	10.0	3.2
363.0	109.1	108.3	14.6	4.0
382.7	104.6	103.7	20.7	5.0
362.9	108.5	107.2	14.8	3.7
322.8	108.8	108.5	7.3	1.9
303.4	108.7	108.2	4.7	1.5
303.4	108.1	107.7	5.1	1.5
271.0	109.0	107.9	4.0	1.1
241.7	108.6		3.3	

C_{94} (annealed)

T	m=1	m=2	I_1	I_2
381.8	109.6	106.9	1990	494
362.6	113.0	110.4	1600	485
337.3	115.8	112.6	1240	404
308.0	116.0		1060	
382.9	109.0		2050	
386.1	107.7		2030	
386.6	106.0			

TABLE 3. *Calculated* n-*paraffin (001)-spacings in Å (at room temperature)*

Phase	Compound n-$C_{36}H_{74}$	Compound n-$C_{44}H_{90}$	Compound n-$C_{94}H_{190}$
Orthorhombic [a]	47.6 [10]	58.3 [15]	122 [17]
Monoclinic, M_{012}	46.1	56.5	118
M_{101}	45.0	55.2	115
M_{011}	[b] 42.3	[c] 51.9	109
M_{201}	[b] 39.3	48.1	101

[a] The orthorhombic spacings are taken from the literature; the monoclinic values are based on the orthorhombic unit cell with

$$a = 7.42 \text{ Å}, \quad b = 4.95 \text{ Å}, \quad \text{and} \quad c_s = 2.54 \text{ Å}.$$

[b] Ohlberg [21] has observed spacings of 47.60, 42.22, and 39.08 Å in hexatricontane.
[c] Ränby et al. [15], have observed a spacing of 52.2 Å in their sample of tetratetracontane.

Also in table 2 are reported the results obtained on C_{94} (m.c.). The intensities, listed in the order in which they were obtained, are reversible with temperature. The d-spacing of 100.3 Å (second order) shows that the sample was initially in the M_{201} monoclinic phase after rapid cooling from the melt. On heating to 323 K the sample was found to give a second order spacing of 107.2 Å which may indicate a phase transformation to a M_{011} phase. The second order spacings from this sample are plotted in figure 4. Comparison of spacings obtained with pinhole collimation, using film exposure, and with our camera on the same melt crystallized sample of n-$C_{94}H_{190}$ at room temperature show that these second order spacings are not in error from slit smearing by more than 0.6 Å.

The data taken on C_{94} (s.c.) and C_{94} (annealed) are likewise given in table 2. Second order values of the (001) spacing as a function of temperature are shown in figure 4 for these samples. For the orthorhombic C_{94} (s.c.) an irreversible decrease in the background intensity occurred on heating to 324 K; although the sample showed no evidence of a phase change until it was heated above 338 K.

The (00l) spacings of C_{94} (annealed) indicated that a conversion from the initial orthorhombic phase had taken place upon heating to 381.8 K. (No separate d-spacing characteristic of the orthorhombic phase was found.) Although the sample appeared to contain a mixture of phases, the intensity and value of the d-spacing were reversible after cooling, as may be seen by comparison of lines 1 and 5 of the data for this sample in table 2.
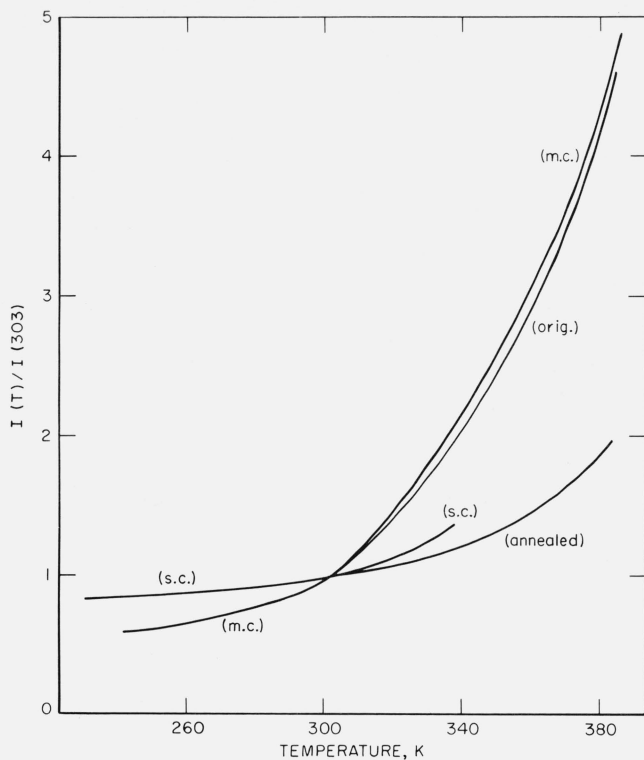
FIGURE 5. *A summary plot of the integrated x-ray diffraction intensity of the (001) maximum at temperature* T *relative to that at 303 K.*

Results on four different samples of $n\text{-}C_{94}H_{190}$ are shown.

A summarizing plot of the first order diffraction intensities as a function of temperature from the four $n\text{-}C_{94}H_{190}$ samples is given in figure 5, where the intensities are relative to the values at 303 K. The ratios were obtained from smoothed plots of the measured integrated intensities, assumed to be continuous in the temperature range of observation.

3.2. Tetratetracontane

The results of the diffraction scans on $n\text{-}C_{44}H_{90}$ are listed in table 4 and three of the as-observed scans are plotted in figure 6. The (001) spacing of the solution crystallized sample, 51.8 Å, is almost identical with that calculated for the M_{011} monoclinic phase (see table 3). When the sample was heated above 333.3 K, the (001) spacing increased abruptly to about 54.5 Å, showing the presence of a solid-solid phase transformation. The change in the d-spacing was also accompanied by a large increase in its integrated intensity. Table 3 suggests that the new phase might be an M_{101} monoclinic. After heating to a maximum temperature of 356.5 K and then cooling to room temperature, the primary d-spacing was 58.0 Å, showing that most of the sample had converted to the orthorhombic phase ($d = 58.3$ Å [15]). However, part of the sample transformed again into its original state on cooling as may be seen from the dashed curve in figure 6.
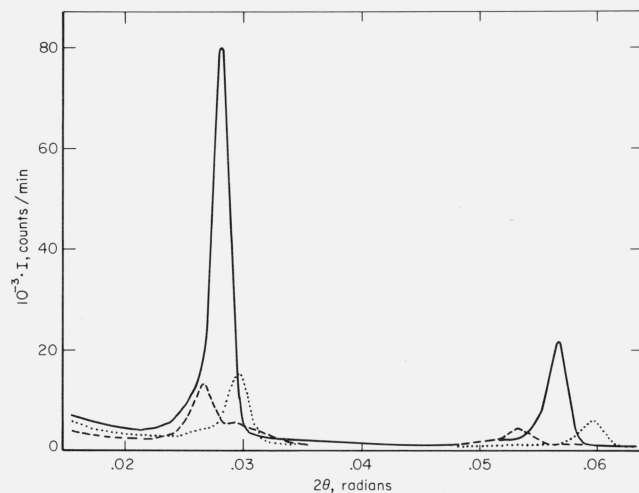

FIGURE 6. *The observed x-ray diffraction intensity from* $n\text{-}C_{44}H_{90}$ *at three temperatures as a function of scattering angle.*

The dotted line is with the sample initially at a room temperature of 297.2 K; the solid line with the sample at 356.5 K; and the dashed line again at room temperature, 296.2 K.

TABLE 4. *Integrated intensities and values of (001) spacings for* $n\text{-}C_{44}H_{90}$, *listed in the order observed*

T	(001) spacing		I_1	I_2
	$m=1$	$m=2$		
K	Å	Å	$cts \cdot rad/min$	$cts \cdot rad/min$
297.2	52.2	51.8	39	15.8
313.1	52.1	51.8	40	17.0
333.3	52.2	51.8	43	21.3
352.2	54.8	54.3	128	38.7
356.5	54.9	54.5	173	49.7
347.7	55.0	54.7	145	51.7
333.3	56.1	55.9	96	39.2
296.2	58.2	58.0	46	16.6

3.3. Hexatriacontane

Our $n\text{-}C_{36}H_{74}$ samples showed a rather complex diffraction pattern, especially at higher temperatures. Figure 7 is a plot of the diffraction scans from a melt-crystallized specimen of the purified sample taken at 296 and 344 K. The numerous subsidiary peaks to the left of the primary maximum make integration of the intensity of the latter uncertain.[4] For this reason, we report only the peak intensity above the background in table 5. Very similar results were obtained on both the purified sample and on the original melt-crystallized material. Table 5 also gives the peak intensities and (001) spacings of the quenched $n\text{-}C_{36}H_{74}$ samples from toluene and sprayed alcohol solution. The changes in d-spacing and peak intensity were found to be reversi-

---

[4]Prof. E. W. Fischer (University of Mainz) has suggested that the subsidiary peaks result from a small number of large crystals which give nonuniform smearing.
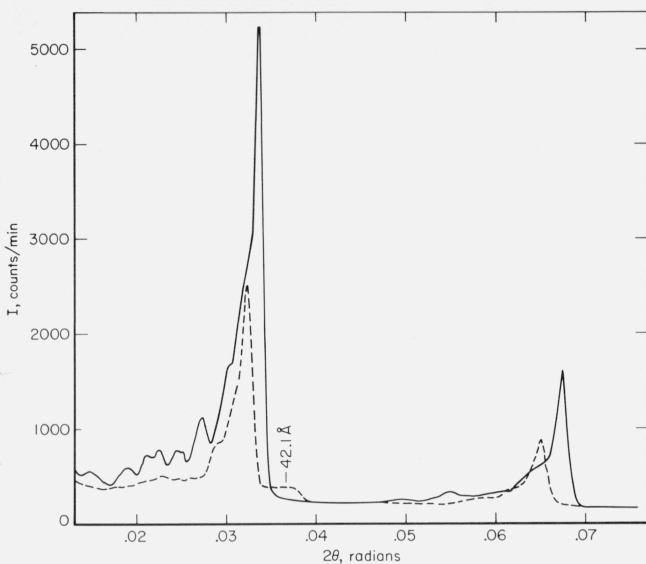
FIGURE 7. *The observed x-ray diffraction intensity from purified* n-$C_{36}H_{74}$ *at 344.2 K (solid line) and at room temperature, 296.4 K, (dashed line) as a function of the scattering angle.*

TABLE 5. *Peak intensities and values of (001) spacings for* n-$C_{36}H_{74}$ *listed in the order observed*

	Original (m.c.)			
T	(001) spacing		I_1	I_2
	$m=1$	$m=2$		
K	Å	Å	cts min^{-1}	cts min^{-1}
297.2	48.1		2170	
342.2	47.0	46.7	5740	1610
329.9	47.9	47.3	5360	1680
297.2	48.1	47.8	2500	900
	Purified (m.c.)			
297.2	48.0		1540	
344.2	45.9	45.8	4580	1370
322.5	47.0	47.0	3160	1050
296.4	47.6	47.4	2220	680
	From Toluene			
297.2	48.0	47.5	579	148
335.7	47.2	47.1	834	196
345.3	45.9	45.6	1421	226
	From sprayed ethanol			
297.2	48.1	47.7	237	76
345.4	46.3	46.2	570	138

ble with temperature. Also, the magnitude of the intensity change was found to be similar to the other n-$C_{36}H_{74}$ samples.

The change in the orthorhombic d-spacing with temperature, given in table 5, is similar to that reported by Barbezat-Debreuil [20]. It would appear to be a result of a partial phase transition to either the M_{011} or M_{101} monoclinic phase (or both), such as has been described by Keller [19].

The melt-crystallized n-$C_{36}H_{74}$ at room temperature is in a state very similar to that which n-$C_{44}H_{90}$ was in after the latter was heated and then cooled to room temperature. In both cases the principle maximum is from the orthorhombic phase but a small part of the sample is in the M_{011} monoclinic phase, which in the case of n-$C_{36}H_{74}$ Ohlberg [21] has shown to be the more stable phase. The simultaneous occurrence of two different phases in a given sample—which has been observed in all three of our n-paraffins—indicates some difficulty in the initiation and/or propagation of the more stable phase. Keller [19] has observed the presence of all the different monoclinic phases listed in table 3 as well as several triclinic phases in single crystals of n-$C_{36}H_{74}$ which were originally orthorhombic.

Our observations indicate that neither the intensity change with temperature nor the magnitude of the (00l) spacing is particularly sensitive to the purity of the n-$C_{36}H_{74}$. In contrast to the commonly held point of view [9, 21, 22] that pure n-$C_{36}H_{74}$ should crystallize in the monoclinic form, we found that both our purified and impure as-received samples (when crystallized from the melt) were predominantly in the orthorhombic phase. Moreover the impure as-received n-$C_{36}H_{74}$ was entirely in the M_{011} monoclinic phase before being melted. For these reasons we do not consider the phase or thermodynamic state of this material to be solely controlled by the chemical purity of the sample and suggest that the crystallization conditions and history of the sample are important factors in determining the phase observed at room temperature.

4. Discussion

It is clear from the data shown in figures 4, 6, and 7 that most of our n-paraffin systems are mixtures of the various crystalline phases. However, the generally observed increase in the intensity of the long-spacing with increasing temperature also occurred in the pure orthorhombic phase of n-$C_{94}H_{190}$ prepared from dilute solution. This leads us to consider several possible mechanisms through which the intensity could increase in a single crystalline phase. The mixed phases will be discussed subsequently.

4.1. Integrated Intensities and Thermal Vibrations

For a crystalline system composed of units having a scattering factor $F(\theta_B, T)$ the integrated intensity $I(\theta_B, T)$ for a diffraction maximum from a powder is given by [6]

$$I(\theta_B, T) = \text{const.} \, |F(\theta_B, T)|^2 p \frac{1+\cos^2 2\theta_B}{\sin^2\theta_B \cos\theta_B}, \quad (1)$$

where 2θ is the scattering angle, T the Kelvin temperature and p the multiplicity of the Bragg reflection at θ_B. For the low-angle maxima in our samples p is constant. Suppose there are a total of L CH$_2$ units in a platelet. Then the scattering factor, $F(\theta, T)$ for this platelet is approximately:

$$F(\theta, T) = \sum_{j=0}^{L-1} f_{CH_2} e^{iks \cdot \mathbf{r}'_j(T)}, \qquad (2)$$

where [5] f_{CH_2} is the scattering factor for a CH$_2$ unit and we consider $f_{CH_3} \cong f_{CH_2}$.

a. Debye-Waller Factor

In the case where the oscillations of the CH$_2$ groups in a paraffin chain are independent and each oscillator possesses the same mean energy, then one has:

$$|F(\theta, T)|^2 = e^{-2(MT)}|F_0(\theta, T)|^2. \qquad (3)$$

The Debye-Waller factor is $e^{-2M(T)}$ and $F_0(\theta, T)$ is the scattering factor for the platelet without vibrations. The quantity $M(T)$ in the Debye-Waller factor [6] is given by:

$$M(T) = 8\pi^2 \overline{u^2(T)} \left(\frac{\sin\theta}{\lambda}\right)^2. \qquad (4)$$

The mean-square displacement of a CH$_2$ unit along s is $\overline{u^2(T)}$. The term $\overline{u^2(T)}$ increases approximately linearly with temperature [6, 23] so that one would expect the intensity of the maxima to decrease with increasing temperature.

One can estimate an upper bound on $\overline{u^2(T)}$ and thereby $M(T)$ as follows: Since the bonding is stronger along the paraffin chain than it is perpendicular to it, $\overline{u_\parallel^2} < \overline{u_\perp^2}$ (where $\overline{u_\parallel^2}$ is along and $\overline{u_\perp^2}$ is perpendicular to the chain). Bunn [8] has found that $8\pi^2 \overline{u_\perp^2}$ is about 5 Å^2 at room temperature for the wide angle diffraction from crystalline polyethylene. The factor $\left(\frac{\sin\theta}{\lambda}\right)^2$ for the low-angle maxima is about 10^{-4} Å^{-2} for n-C$_{36}$H$_{74}$ and about 10^{-5} Å^{-2} for n-C$_{94}$H$_{190}$ at the first order. Then $M(295\text{ K})$ is about 5×10^{-4} Å^{-2} and $M(385\text{ K})$ about 7×10^{-4} Å^{-2} at most, so that $e^{-2M(T)}$ is 1.000 within 0.1 percent over our temperature range of interest.

b. Thermal Diffuse Scattering

While independent vibrations of the —CH$_2$— units are considered in the Debye-Waller factor, correlated vibrations such as occur in long wavelength phonons in these solids are accounted for in the thermal diffuse scattering. For discussion on this topic, the reader is referred to Warren [24] and to James [6].

---

[5] $k = \dfrac{2\pi}{\lambda}$; $s = \hat{s}_i - \hat{s}_o$, $|s| = 2\sin\theta$ where $\hat{s}_i$ is the unit vector of the scattered wave, $\hat{s}_0$ the unit vector for the incident wave; $\mathbf{r}'_j$ is the vector distance from an origin to the jth CH$_2$ unit in the platelet.

Shinomura et al. [5], have attributed the origin of the low-angle maxima in several polymers to such correlated vibrations or elastic waves, with a wavelength of twice the lamellar repeat distance. The multiple peaks in the intensities were attributed to harmonics of these waves.

While the intensity of the thermal diffuse scattering increases with increasing temperature (approximately linearly for kT much larger than the energy of the phonons), these maxima are usually broader and weaker than the Bragg maxima [6]. The first order thermal diffuse scattering has maxima at angles such that

$$\frac{2\sin\theta}{\lambda} = \frac{m}{d_{001}} \pm \frac{1}{\Lambda}, \qquad (5)$$

where m is the order of the (001) maxima and Λ is the wavelength of the phonon. For a broad distribution of phonon wavelengths one expects—based on eq (5)—that the intensity due to these vibrations is scattered over a wider angular range than the Bragg maximum. We expect that much of this diffuse scattering is subtracted in our background corrections.

We note that for many solids the contribution of thermal vibrations to the integrated intensity over the Bragg maxima is adequately accounted for by the Debye-Waller factor, i.e., by independent oscillations of the scattering units. This implies that the contribution of longer wavelength phonons is not a dominant component of the integrated intensity over a maximum. The vibrations that affect the thermal diffuse scattering for a given Bragg diffraction maximum have a component of their displacements along s for that maximum. For the low-angle maxima, some of the relevant vibrations have been studied by Schaufele and Shimanouchi [25] in their examination of the Raman spectra of n-C$_{36}$H$_{74}$, n-C$_{44}$H$_{90}$, and n-C$_{94}$H$_{190}$. Based on the vibrational frequencies they reported, we note that a very substantial fraction of the molecules in these systems are already excited at room temperature so that we expect no abnormally large contribution from these vibrations to the integrated intensity. It is of course difficult to estimate quantitatively the contribution of all the allowed vibrations to the intensities.

4.2. Single Crystal Versus the Mosaic Crystal

As discussed in considerable detail by James [6] and by Warren [24], the integrated intensities for diffraction maxima of nearly perfect crystals can be substantially smaller than is the case for the ideally imperfect or mosaic crystalline system. The essential idea is that rescattering processes in the more perfect crystalline system lead to wave cancellation, so that the intensities are no longer simply proportional to the volume of the irradiated sample. In the mosaic system this rescattering is interrupted by imperfections so that the process of wave cancellation is reduced. The question arises as to whether the systems we have studied were sufficiently imperfect or mosaic to begin

with or whether temperature induced defects changed the degree of perfection.

It was observed that in the solution-grown sample of n-$C_{94}H_{190}$, most of the growth spirals were no thicker than 20 layers. Yet this sample still displayed an intensity change with temperature, which fact argues against any extinction effects in that sample. A calculation of the relative intensity of the first and second orders of the (001) spacing for an unoriented sample under our camera conditions gives an I_2/I_1 of 0.35, which is the same as that observed for our melt-crystallized n-$C_{94}H_{190}$. Since primary extinction reduces the intensity of the first order maximum to a greater extent than the second order, we conclude that this sample did not show extinction effects. Similarly, the data shown in table 5 for n-$C_{36}H_{74}$ quenched in toluene and sprayed from ethanol also shows an intensity increase with temperature. However, such drastic treatments should surely produce very imperfect crystals having no extinction. Based on these observations, we believe that the intensity changes we have observed are not dominated by extinction effects.

4.3. The (00*l*) Structure Factor

Suppose there are N paraffin molecules in a platelet, which we have chosen as the unit of structure. Since the factor [6] $e^{iks \cdot r(T)}$ in eq (2) only involves the projection of r_j onto s, for the (00*l*) maxima, one may sum eq (2) over molecules, so that one has (in the plane wave approximation),[7]

$$F(\theta, T) = N \sum_{j=0}^{n} f_{CH_2} e^{iks \cdot r_j(T)}, \qquad (6)$$

where $n + 1 = L/N$ is the number of units in one molecule.

One may define a molecular scattering factor $F'(\theta, T)$ by the relationship $F(\theta, T) = NF'(\theta, T)$. From eq (6), for the orthorhombic crystalline phase, one has for $F'(\theta, T)$:

$$F'(\theta, T) = f_{CH_2} e^{ik(\sin \theta)nx_0} \frac{\sin [k(\sin \theta)(n+1)x_0]}{\sin [k(\sin \theta)x_0]} \qquad (7)$$

where x_0 is the projection of a CH_2 repeat distance onto s (1.27 Å). The magnitude of this (00*l*) scattering factor agrees with the scattering factor of Müller for orthorhombic n-$C_{29}H_{60}$ [11] and of Teare for orthorhombic n-$C_{36}H_{74}$ [10]. From eq (6), $F'(\theta, T)$ becomes for the monoclinic forms of the n-paraffins in the angular range of our interest,

$$F'(\theta, T) \cong (2f_{CH_2}) e^{ik(\sin \theta)nx_M} \frac{\sin [k(\sin \theta)(n+1)x_M]}{\sin [k(\sin \theta)2x_M]} \qquad (8)$$

where $2x_M$ is the projection of a C_2H_4 repeat distance onto s. The magnitude of $F'(\theta)$ given in eq (8) agrees with the scattering factors observed by Shearer and Vand [9] for monoclinic n-$C_{36}H_{74}$.

If we define an interlamellar distance $A(T)$ as $d(T) = (n+1)x + A(T)$ and limit eqs (7) and (8) to the Bragg maxima ($m\lambda = 2d \sin \theta_B$), we have:

$$|F'(\theta_B, T)| \cong f_{CH_2} \frac{\sin [\pi m A_0/d_0]}{\sin [\pi m x_0/d_0]} \cong f_{CH_2} \frac{A_0}{x_0} \qquad (7a)$$

for the orthorhombic phase, and,

$$|F'(\theta_B, T)| \cong (2f_{CH_2}) \frac{\sin [\pi m A_M/d_M]}{\sin [\pi m 2x_M/d_M]} \cong f_{CH_2} \frac{A_M}{x_M} \qquad (8a)$$

for the monoclinic phase (when $d \gg x$).

One notices that for either crystalline phase, the wave from a single molecule is mostly cancelled and depends primarily on the interlamellar distance A. From eq (1), one has

$$\frac{I(\theta_B, T_2)}{I(\theta_B, T_1)} = \left[\frac{F'(\theta_B, T_2)}{F'(\theta_B, T_1)}\right]^2 \cong \left[\frac{A(T_2)}{A(T_1)}\right]^2. \qquad (9)$$

Here we assume the change in A with temperature is much larger than the change in x, since the carbon atoms are covalently bonded along the chain.

a. Interlamellar Expansion

The question arises as to whether a simple interlamellar expansion with temperature could explain the intensity effects we have observed. The magnitude of this effect on $I(\theta_B, T)$ may be estimated as follows: If one assumes that the interlamellar distance expands approximately as the a-dimension of the subcell (of the a, b and c subcell dimensions, the a expands most), then over a 100 K temperature range (e. g., 240 to 340 K), the expansion is about 0.20 Å [26]. Since the excess distance between terminal methyl groups—the interlamellar distance—is 1.98 Å for the orthorhombic n-paraffins and 2.93 Å for the M_{011} monoclinic phases [27], then from eq (9), one estimates that the intensity increase due solely to interlamellar thermal expansion is no more than 21 percent over this temperature range. The observed intensity increase over the range $231 \leq T \leq 338$ K, shown in table 2, for the orthorhombic phase of n-$C_{94}H_{190}$ is 59 percent. Thus, it appears that the intensity change with temperature does not result solely from a simple interlamellar expansion.

Let us now consider additional mechanisms by which the structure factor and thereby $A(T)$ can change with temperature. One point of view for polyethylene is considered briefly below. As far as the n-paraffins are concerned, two processes are suggested. The first, considered in section (4.3b) below, is that of chain defects or kinks, which lead to vacancy formation on the surface of the platelet and thereby essentially an

---

[6] We replace the distance vector $r_j'(T)$ with $r_j(T)$ for the nonvibrating repeat unit, since the Debye-Waller factor is negligible at low angles.

[7] In the Fresnel or spherical wave treatment [6], $F(\theta, T) = \frac{const.}{\sin \theta} N \sum_{j=0}^{n} f_{CH_2} e^{iks \cdot r_j(T)}$.

increase in A. The second, discussed in section (4.3c), is that of a tilting of the molecule via a phase transformation, which also can lead to an increase in A from poorer packing of the methyl groups or possibly from void formation at the lamellar surface.

The essential idea put forward by Fischer et al. [3], and by Schultz et al. [28], to explain the temperature dependence of the intensity of the low-angle maxima in polyethylene (see fig. 8), is that the lamellar surface is disordered or amorphous and that the size of this disordered region increases reversibly with increasing temperature because of a gain in entropy. According to their discussion, if the electron density difference between the amorphous and crystalline regions changes little with temperature, then the low-angle diffraction intensity will increase as the size of the interlamellar region increases. However, we do not consider an amorphous lamellar surface, such as described by Fischer et al. and Schultz et al., appropriate for the n-paraffins since these systems are known to be polymorphic. For example, Templin [29] reported three crystalline phases for n-$C_{36}H_{74}$ (observed dilatometrically) above 333 K. Rånby et al. [15] found two phases in n-$C_{44}H_{90}$. Simi-larly, Khoury [18] has observed three forms of n-$C_{94}H_{190}$ (one orthorhombic and two monoclinic). The differences among the various monoclinic phases and the orthorhombic phase for the long-chain n-paraffins is only in the end-group packing—these systems all have essentially the same orthorhombic subcell (see also table 2). Now, if the surfaces of these n-paraffin lamellae were disordered, crystalline phases which are different only in end-group packing would not exist, which is contrary to experimental observation. Thus we are led to consider models other than an amorphous lamellar surface to explain the intensity changes.

b. Chain Defects

Due to the almost total cancellation of the wave scattered from a long-chain n-paraffin molecule for the $(00l)$ maxima and the sensitivity of the intensity to the interlamellar distance, there is a mechanism by which certain types of chain defects can increase the intensity of these maxima.

The class of defects we are concerned with have been described by Reneker [30] and more recently by Pechold and Blasenbrey [31]. Keith and Passaglia [32] have considered similar chain defects in the form of dislocations and glide in paraffin crystals (see also Predecki and Statton [33]). These defects can essentially be considered—in the case of the $(00l)$ low-angle maxima—as the formation of a point vacancy at the surface of the platelet and the superposition of a unit along the chain (fig. 9). Insofar as the lamellae do not collapse into the surface voids, the point vacancies lead to an increase in the effective interlamellar distance.

FIGURE 9. *Schematic diagram of a paraffin lamella with defects leading to surface vacancies.*
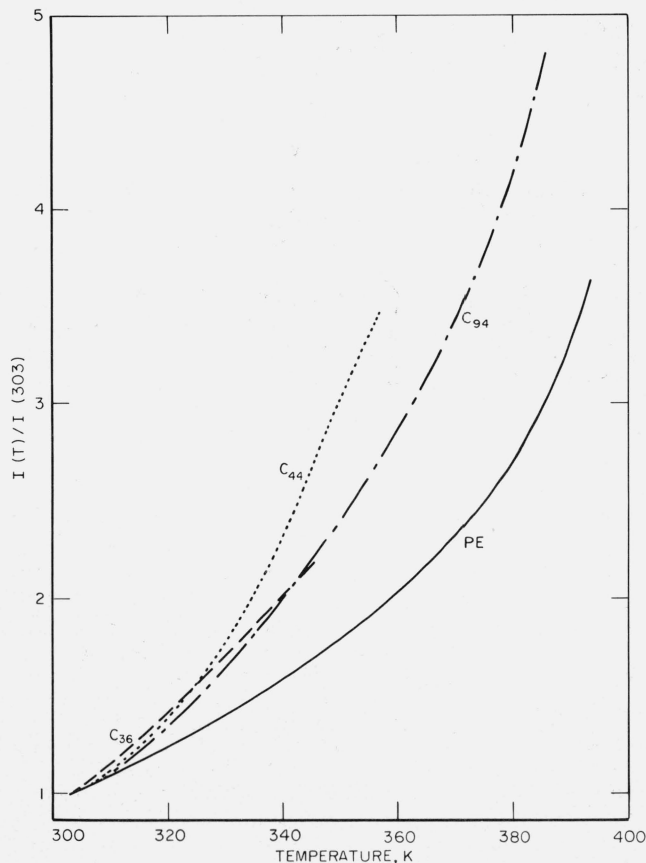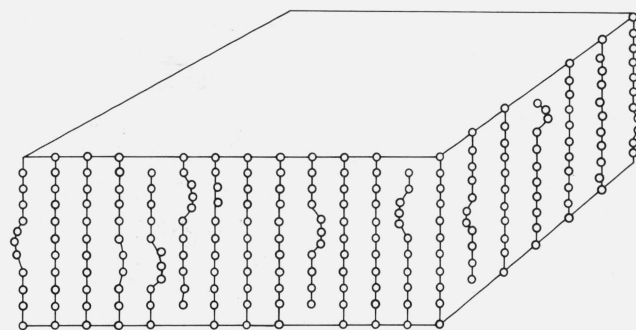

FIGURE 8. *A comparison of the relative x-ray diffraction intensity from the (001) maximum for three of our samples with data from the literature on linear polyethylene.*

Dashed line, n-$C_{36}H_{74}$ (purified); dotted line, n-$C_{44}H_{90}$ cooled from 356.5 K to room temperature; alternate dash and dot, n-$C_{94}H_{190}$ (orig); and solid line, data of Fischer et al., on polyethylene [3].

In order to estimate the fraction $\beta(T)$ of defect chains in a platelet, we write the structure factor $F(\theta, T)$ so as to include these chains. We assume the kink formation creates a surface vacancy the size of one —CH_2— unit and that there is only one kink per defect chain. For the moment allowing each kink to be in the qth position, then from eq (6) one has:

$$F(\theta, T) \cong N_1(T) \sum_{j_1=0}^{n} f_{CH_2}\, e^{iks \cdot r_{j_1}}$$

$$+ N_2(T) \left[\sum_{j_2=1}^{n} f_{CH_2} e^{iks \cdot r_{j_2}} + f_{CH_2} e^{iks \cdot r_q} \right]$$

$$+ N_3(T) \left[\sum_{j_3=0}^{n-1} f_{CH_2} e^{iks \cdot r_{j_3}} + f_{CH_2} e^{iks \cdot r_q} \right], \quad (10)$$

where there are N_1 nondefect chains, and $(N_2 + N_3)$ defect-containing chains. We allow for the vacancy at either the top or bottom of the platelet.

If we assume each platelet in a stack has the same number of molecules and the defect chains are in thermal equilibrium with the nondefect chains, then each platelet has the same number of defect chains. Since the distance vectors r_j from the origin to the —CH₂— units of each chain (with or without a kink defect) are projected onto s and since we are only concerned with $(00l)$ maxima, then there is no effect on $F(\theta, T)$ of the location of a defect chain in a platelet. For this reason the scattering factor of every platelet in a stack is identical and only depends on the concentration of the defect chains.

Summing eq (10), one has:

$$F(\theta, T, q) \cong N_1(T) f_{CH_2} e^{ik(\sin\theta)nx} \frac{\sin[k(\sin\theta)(n+1)x]}{\sin[k(\sin\theta)x]}$$

$$+ 2N_2(T) f_{CH_2} \left[e^{ik(\sin\theta)nx} \frac{\sin[k(\sin\theta)nx]}{\sin[k(\sin\theta)x]} \right.$$

$$\left. + e^{ik(2\sin\theta)qx} \right] \quad (11)$$

for the case $N_2 = N_3$.[8] We note that $|F(\theta, T, q)|^2$ depends on q and is greatest when the superimposed group is at the center of a chain and least when near a methyl end-group.

If instead of allowing every superimposed CH₂ unit to be at position q in the defect chain, we allow the kink to be located anywhere along a chain with equal probability, then the second expression in eq (11) becomes a sum over the positions q. One can then write eq (11) as:

$$F(\theta, T) \cong N_1 f_{CH_2} e^{ik(\sin\theta)nx} \frac{\sin[k(\sin\theta)(n+1)x]}{\sin[k(\sin\theta)x]}$$

$$+ 2N_2 f_{CH_2} e^{ik(\sin\theta)nx} \frac{\sin[k(\sin\theta)nx]}{\sin[k(\sin\theta)x]} \left[1 + \frac{1}{n} \right] \quad (12)$$

Defining $\beta(T)$ as $2N_2 = \beta(T)N$ where $(N_1 + 2N_2) = N$, then for orthorhombic n-$C_{94}H_{190}$ one has at the first order Bragg maximum:

$$F(\theta_B, T) \cong \frac{N f_{CH_2}}{x} \left[e^{i(A+x)/d} \right] [(1-\beta)A + \beta(A+x)]$$

$$(13)$$

so that the intensity becomes (c.f. eq (1))

[8] We have taken $\cos[k(\sin\theta)x] \cong 1$ in our range of 2θ.

$$I(\theta_B, T) \cong \text{const.} \frac{N^2 f_{CH_2}^2}{x^2} (A + \beta x)^2 p \frac{1 + \cos^2 2\theta_B}{\sin^2 \theta_B \cos \theta_B}$$

$$(14)$$

If the defect-containing chains are in a Boltzmann equilibrium with the nondefect chains, then for a change in integrated intensity of 38 percent—which is the excess over the contribution due to thermal expansion estimated earlier—one arrives at an energy of 4100 cal/mol defects. Reneker has estimated this energy as 4600 cal/mol defects [30] from steric considerations. We conclude that for the solution-crystallized orthorhombic n-$C_{94}H_{190}$ the intensity change with temperature is consistent with thermal expansion of the interlamellar region and a thermal generation of vacancies, e.g., via kink formation.

We note that the maximum increase in $I(\theta_B, T)$ of eq (14) is a factor of 2.6, assuming the size of a vacancy is 1.27 Å. Also the intensity change is enhanced if most of the kinks occur at the same position in the molecules rather than at random along the chain. This would involve an interaction or cooperative effect with these defects, as for example would occur in a glide plane. However, the larger intensity changes found for C_{94} (orig.) and C_{94} (m.c.) suggest that possibly additional mechanisms are operating. One such possibility is considered below.

c. Mixtures of Phases

In view of the fact that all of the systems we have studied are polymorphic and that in the temperature range of our observations the systems must be experiencing solid-solid transitions, which can be quite slow as has been observed by Ohlberg [21], it seems likely that some of our observed intensity change is associated with these transitions.

The end-group packing and thereby the interlamellar distance is different for the various crystalline phases [27], which fact leads one to expect that the intensity of the $(00l)$ maxima should change when a system undergoes a transition. Moreover, if the transition were not complete or abrupt, so that platelets of one phase were in contact with those of a different phase, the intensity change could be enhanced due to further complications in end-group packing. For example, the $(00l)$ planes in M_{011} and M_{201} monoclinic phases have different subcell areas, which would lead to a mismatch of the terminal CH_3-groups when these platelets are adjacent in a stack. This is so even with good packing of the lamellae. In addition to these effects, there is the possibility of void formation at the surface of the lamellae when changes of 2 to 20 Å occur in the long-spacings due to a solid-solid transition. It seems the system might experience collapse difficulties which could give rise to a substantially larger interlamellar distance than occurs in the situation with good end-group packing. An assessment of the magnitude of these effects would indeed be difficult. However, since the intensity of the low-angle maxima is so sensitive to this interlamellar dis-
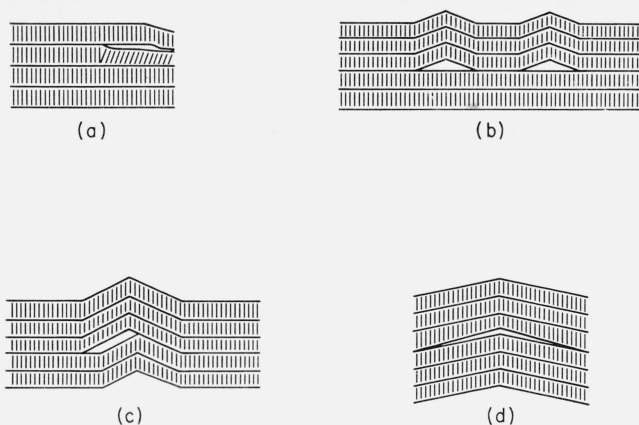
FIGURE 10. *Schematic diagrams of transitions in stacks of n-paraffin lamellae with incomplete collapse leading to surface vacancies.*

tance, it is plausible that these processes are contributing to the intensity changes observed with temperature in those samples where phase transitions are occurring.

We indicate schematically in figure 10 surface vacancies which might arise from solid-solid phase transitions. In figures 10a, b, and c are shown vacancies which could occur during the transition from the orthorhombic to the monoclinic phase. In figure 10d is shown the situation after the transition when the subsequent collapse is incomplete or for imperfect packing of end groups. This does raise the question of the reversibility of the intensity change with temperature, since one might expect the vacancies arising from the transitions to occur irreversibly. For example, Keller [19] and Baltá Calleja [34] have observed irreversible morphological changes on the surfaces of n-paraffin lamellae after heating. But, the fact that the low-angle diffraction intensities change so substantially in the regions where these systems undergo solid-solid transitions suggests that they are interrelated.

5. Conclusions and Summary

We have seen that the intensity of the low-angle x-ray diffraction maxima increases reversibly with increasing temperature for the n-paraffins which we examined. The magnitude of this intensity change was found to depend on the structure arising from the sample preparation (e.g., melt-crystallized versus solution-crystallized) in the case of n-$C_{94}H_{190}$, but was rather insensitive to physical state or purity in n-$C_{36}H_{74}$. All the samples experienced solid-solid phase transitions at temperatures below their melting points. From the observed $(00l)$ spacings, the transitions did not appear sharp, as might be expected for a first-order transition. However, part of the gradual change in d_{00l} may have resulted from the slow elimination of microvoids which were generated during the transition. Since the structure factor of these long-chain molecules is very sensitive to the interlamellar distance, we were led to consider temperature-dependent mechanisms which change this distance. These include: (a) thermal expansion of the interlamellar distance; (b) defects

which involve a contraction of the chains and give rise to surface vacancies, such as Reneker defects or glide planes; and (c) phase transitions leading to poorer packing of methyl groups in adjacent lamellae or void formation. The observations for orthorhombic n-$C_{94}H_{190}$ are consistent with processes (a) and (b). We suggest that the intensity changes for the remaining samples can be accounted for by all three processes.

6. References

[1] Geil, P. H., Polymer Single Crystals (John Wiley and Sons, N.Y., 1963).
[2] Statton, W. O., J. Polymer Sci. **28**, 423 (1958).
[3] Nukushina, Y., Itoh, Y., and Fischer, E. W., Polymer Letters **3**, 383 (1965).
[4] O'Leary, K., and Geil, P., J. Macro. Sci. **1B**, 147 (1967).
[5] Shinomura, M., Chiba, A., and Furuichi, J., Reports Prog. Polymer Physics Japan **9**, 187 (1966).
[6] James, R. W., Optical Principles of the Diffraction of X-Rays, (Cornell Univ. Press, Ithaca, N.Y., 1965).
[7] Waller, I., and James, R. W., Proc. Roy Soc. Lond. **A117**, 214 (1927). Batterman, B. W., Phys. Rev. **126**, 1461 (1962). Flinn, P. A., and McManus, G. M., Phys. Rev. **132**, 2458 (1963). Sparks, C. J., Jr., and Borie, B. S., Adv. in X-Ray Analysis **6**, 177 (1963).
[8] Bunn, C. W., Trans. Faraday Soc. **35**, 482 (1939).
[9] Shearer, H. M. M., and Vand, V., Acta Cryst. **9**, 379 (1956).
[10] Teare, P. W., Acta Cryst. **12**, 294 (1959).
[11] Müller, A., Proc. Roy. Soc. **120**, 437 (1928).
[12] Khoury, F., J. Appl. Phys. **34**, 73 (1963).
[13] Reinhard, R. R., Ph. D. Thesis, The Penn. State Univ. (1961).
[14] Bridgman, P., Proc. Am. Acad. Arts Sci. **60**, 305 (1925). Horton, A. T., and Glasgow, A. R., Nat Bur. Stand. (U.S.) **69C** (Eng. and Instr.) No. 3, 195–198 (July–Aug. 1965).
[15] Rånby, B. G., Morehead, F. F., and Walter, N. M., J. Poly. Sci. **44**, 349 (1960).
[16] Clark, S. G., M. S. Thesis, The Penn. State Univ. (1956).
[17] Wyckoff, H. W., Khoury, F., and Hyndman, D., Bull. Am. Phys. Soc. **7**, 206 (1962).
[18] Khoury, F., Am. Chem. Soc. Polymer Preprints **3**, 104 (1962).
[19] Keller, A., Phil. Mag. **6**, 329 (1961).
[20] Barbezat-Debreuil, S., Comptes Rendus **246**, 2907 (1958).
[21] Ohlberg, S. M., J. Phys. Chem. **63**, 248 (1959).
[22] Piper, S. H., and Malkin, T., Nature **126**, 278 (1930).
[23] Becka, L. N., and Cruickshank, D. W. J., Proc. Roy. Soc. **A273**, 455 (1963).
[24] Warren, B. E., X-Ray Diffraction (Addison-Wesley Pub. Co., Reading, Mass., 1969).
[25] Schaufele, R. F., and Shimanouchi, T., J. Chem. Phys. **47**, 3605 (1967).
[26] Cole, E. A., and Holmes, D. R., J. Polymer Sci. **46**, 245 (1960). Swan, P. R., J. Polymer Sci. **56**, 403 (1962).
[27] Broadhurst, M. G., Nat. Bur. Stand. (U.S.), **66A** (Phys. and Chem.) No. 3, 241–249 (May–June 1969).
[28] Schultz, J. M., Robinson, W. H., and Pound, G. M., J. Polymer Sci. **A5**, 511 (1967).
[29] Templin, P. R., Ind. Eng. Chem. **48**, 154 (1956).
[30] Reneker, D. H., J. Poly. Sci. **59**, 539 (1962).
[31] Pechhold, W., and Blasenbrey, S., Kolloid Zeitschrift **216** 235 (1967).
[32] Keith, H. D., and Passaglia, E., Nat. Bur. Stand. (U.S.), 68A (Phys. and Chem.) No. 5, 513–518 (Sept.–Oct. 1964).
[33] Predecki, P., and Statton, W. O., J. Appl. Phys. **37**, 4053 (1966).
[34] Baltá Calleja, F. J., Rev. Real Acad. Cienc. Exact. Fis. Nat. Marid **59**, 71 (1965).